

Spectral scaling laws in MHD turbulence simulations and in the solar wind

Stanislav Boldyrev,¹ Jean Carlos Perez,^{1,2} Joseph E. Borovsky,^{3,4} and John J. Podesta³

¹*Department of Physics, University of Wisconsin-Madison, Madison, WI 53706, USA*

²*Space Science Center and Department of Physics,
University of New Hampshire, Durham, NH 03824*

³*Los Alamos National Laboratory, Los Alamos, New Mexico 87545, USA*

⁴*Atmospheric, Oceanic, and Space Sciences Department,
University of Michigan, Ann Arbor, MI 48109, USA*

(Dated: May 18, 2011)

The question is addressed to what extent incompressible magnetohydrodynamics (MHD) can describe random magnetic and velocity fluctuations measured in the solar wind. It is demonstrated that distributions of spectral indices for the velocity, magnetic field, and total energy obtained from high resolution numerical simulations are qualitatively and quantitatively similar to solar wind observations at 1 AU. Both simulations and observations show that in the inertial range the magnetic field spectrum E_b is steeper than the velocity spectrum E_v with $E_b \gtrsim E_v$ and that the residual energy $E_R = E_b - E_v$ decreases nearly following a k_\perp^{-2} scaling.

PACS numbers: 52.35.Ra

Introduction.—Plasma motions in astrophysical systems are usually magnetized and turbulent. At scales larger than characteristic plasma kinetic scales, one-fluid magnetohydrodynamics provides a satisfactory framework for studying such systems [1, 2]. Magnetohydrodynamic turbulence has long been invoked to explain the properties of the solar wind, where velocity and magnetic field fluctuations are measured *in situ* over a wide range of scales [e.g., 3–5]. Recent high-resolution numerical simulations, however, reported intriguing contradictions with the observational data. The Fourier energy spectrum of MHD turbulence obtained from numerical simulations appears to have a different scaling compared to the scaling inferred from observations. This raises some serious questions. Do the numerical simulations correctly represent the physics of solar wind fluctuations and, if so, then why doesn't solar wind turbulence exhibit the same universal scaling found in 3D MHD simulations?

To formulate the problem, we rewrite the incompressible MHD equations in terms of the Elsässer variables,

$$\left(\frac{\partial}{\partial t} \mp \mathbf{v}_A \cdot \nabla\right) \mathbf{z}^\pm + (\mathbf{z}^\mp \cdot \nabla) \mathbf{z}^\pm = -\nabla P, \quad (1)$$

where the Elsässer variables are defined as $\mathbf{z}^\pm = \mathbf{v} \pm \mathbf{b}$, \mathbf{v} is the fluctuating plasma velocity, \mathbf{b} is the fluctuating magnetic field normalized by $\sqrt{4\pi\rho_0}$, $\mathbf{v}_A = \mathbf{B}_0/\sqrt{4\pi\rho_0}$ is the Alfvén velocity corresponding to the uniform magnetic field \mathbf{B}_0 , $P = (p/\rho_0 + b^2/2)$ includes the plasma pressure p and the magnetic pressure, ρ_0 is the constant mass density, and we neglect driving and dissipation terms. The guide field \mathbf{B}_0 can be either imposed by external sources or associated with large scale fluctuations that are almost uniform with respect to the scales of the inertial range. It follows from these equations that for $\mathbf{z}^\mp(\mathbf{x}, t) = 0$, an arbitrary function $\mathbf{z}^\pm(\mathbf{x}, t) = F^\pm(\mathbf{x} \pm \mathbf{v}_A t)$ is an exact nonlinear solution

that represents a non-dispersive Alfvén wave propagating along the direction $\mp \mathbf{v}_A$. Nonlinear interactions are thus the result of collisions between counter-propagating Alfvén wave packets.

Denote by $E^\pm = \langle |\mathbf{z}^\pm|^2 \rangle / 4$ the energies associated with the \pm waves. Those two quantities are independent integrals of motion of the ideal MHD system (1). They are related to the total energy and cross-helicity, $E = E^+ + E^-$ and $H_c = E^+ - E^-$, respectively. Cross-helicity provides a measure of *imbalance* between interacting Alfvén modes; when $H_c \neq 0$ the turbulence is called imbalanced, otherwise it is balanced. The solar wind is essentially imbalanced, as more Alfvén waves propagate away from the sun than toward the sun. In a turbulent state, when energy is supplied to the system at large scales, both E^\pm cascade toward small scales where they are damped by viscosity and resistivity. Theories and numerical simulations of MHD turbulence address the Fourier spectra of the energies $E^\pm(k)$ in the inertial range of scales, that is, scales much smaller than the forcing scales and much larger than the dissipation scales.

According to numerical simulations, statistics of MHD turbulence are highly anisotropic with respect to the local mean magnetic field. It has recently been argued that the field-perpendicular energy spectra of incompressible, homogeneous, strong MHD turbulence scale as $E^\pm(k_\perp) \propto k_\perp^{-3/2}$, in both balanced and imbalanced cases [6–10], and that this scaling is consistent with analytic models [11]. This picture seems however to contradict the observational data of the solar wind, which often find the spectrum of *magnetic field* fluctuations to be consistent with the Kolmogorov scaling $-5/3$ [e.g., 3]. At the same time, recent measurements of *velocity* fluctuations in the solar wind reveal an essentially shallower spectrum, closer to $E_v(k) \propto k^{-3/2}$ [e.g., 12–16]. This mismatch in the spectral scalings motivated our interest

in the problem. To address the problem we notice that there is no strict requirement that the magnetic and velocity fluctuations be in equipartition with each other. Moreover, even though analytic models often appeal to the picture of counter-propagating Alfvén modes, with $\mathbf{v} = \pm \mathbf{b}$, such Alfvén modes are not statistically independent in strong turbulence. This means, in general, that $\langle \mathbf{z}^+ \cdot \mathbf{z}^- \rangle = \langle v^2 \rangle - \langle b^2 \rangle \neq 0$.

We perform a high-resolution numerical study of both balanced and imbalanced MHD turbulence, and concentrate on individual magnetic and velocity spectra. We find that in both cases these spectra are generally not identical. We observe that the so-called residual energy, characterizing the mismatch of the spectra, $E_r(k_\perp) = E_b(k_\perp) - E_v(k_\perp)$, is not universal in that its *amplitude* depends of the driving and the degree of imbalance. The *scaling* of the residual energy is, however, close to $E_r(k) \propto k_\perp^{-2}$ in both balanced and imbalanced runs. In the balanced case this result was first obtained in [7]. While the total energy spectrum is close to $E(k_\perp) \propto k_\perp^{-3/2}$, the presence of residual energy leads to steeper magnetic spectrum and a shallower velocity spectrum in an inertial interval of limited extent. However, since the residual spectrum declines faster than the total spectrum, the universality of the turbulence should be restored asymptotically at large k_\perp , and it can be observed if the inertial interval is large enough.

For a comparison with the solar wind measurements we plot histograms of velocity and magnetic spectral indices measured for individual temporal snapshots in numerical simulations of MHD turbulence. Comparison of the results with analogous histograms obtained from individual solar wind measurements reveals good agreement, indicating that incompressible MHD provides an adequate framework for modeling MHD-scale turbulence in the solar wind.

Numerical simulations.—The universal properties of MHD turbulence are accurately described by neglecting the parallel component of the fluctuating fields, associated with the pseudo-Alfvén mode, e.g., [17–19]. By setting $\mathbf{z}_\parallel^\pm = 0$ in equation (1) we obtain the closed system of equations

$$\left(\frac{\partial}{\partial t} \mp \mathbf{v}_A \cdot \nabla_\parallel \right) \mathbf{z}^\pm + (\mathbf{z}^\mp \cdot \nabla_\perp) \mathbf{z}^\pm = -\nabla_\perp P + \mathbf{f}^\pm + \nu \nabla^2 \mathbf{z}^\pm, \quad (2)$$

in which force and dissipation terms have been added to address the case of steadily driven turbulence, and we assume that viscosity is equal to resistivity. This set of equations is known as the Reduced MHD model (RMHD) [20, 21], appropriate for studying MHD turbulence with a strong guide field, $v_A \gg v_{rms}$. Numerical simulations of full MHD equations show that the universal regime of strong MHD turbulence is reproduced well for $v_A/v_{rms} \geq 5$ [e.g., 7, 9, 22], which is properly

captured by Reduced MHD system (2). RMHD allows one to reduce the number of fields by a factor of two and to speed up the numerical integration. We employ a fully dealiased Fourier pseudo-spectral method to solve equations (2) in a rectangular periodic box, with field-perpendicular cross section $L_\perp^2 = (2\pi)^2$ and field-parallel box size $L_\parallel = (v_A/v_{rms})L_\perp$. The choice of a rectangular box, as discussed in [10, 11], allows for the excitation of elongated modes at large scales, necessary to avoid a long transition region between the forcing scale and the beginning of the inertial range.

The random forcing \mathbf{f}^\pm is applied in Fourier space at wave-numbers $1 \leq k_\perp \leq 2$, $k_\parallel = 2\pi/L_\parallel$. The Fourier coefficients inside that range are Gaussian random numbers with amplitude chosen so that the resulting rms velocity fluctuations are of order unity. The individual random values are refreshed independently for each mode on average every $\tau = 0.1 L_\perp/v_{rms}$. We define the Reynolds number as $Re = (L_\perp/2\pi)v_{rms}/\nu$. In the present simulations, we also introduce correlation between \mathbf{v} and \mathbf{b} , which is achieved by taking \mathbf{f}^\pm as uncorrelated Gaussian random forces with zero mean and variances $\sigma_\pm^2 \equiv \langle |\mathbf{f}^\pm|^2 \rangle$. Denoting $\mathbf{f}_v = \frac{1}{2}(\mathbf{f}^+ + \mathbf{f}^-)$, and $\mathbf{f}_b = \frac{1}{2}(\mathbf{f}^+ - \mathbf{f}^-)$, we obtain that cross-helicity is controlled by $\langle \mathbf{f}_v \cdot \mathbf{f}_b \rangle = \frac{1}{4}(\sigma_+^2 - \sigma_-^2)$. The results presented below have been conducted at numerical resolution of $1024^2 \times 256$ points, which corresponds to the Reynolds number of $Re \approx 5600$. In the imbalanced run, the normalized cross-helicity is $H_c/E \approx 0.6$. The cases were run for up to 200 large-scale eddy turnover times in order to get reliable statistics, see [11].

The results of numerical simulations are presented in Figs. 1 and 2. Two important observations should be made here. First, there is a tendency of magnetic energy to exceed the kinetic energy at large inertial range scales for both balanced and imbalanced cases. The presence of nonzero residual energy was noted in previous studies [e.g., 7, 23]. Comparison of our results with previously available numerical data suggests that the level of residual energy is not universal, rather, it can be affected by the driving and the degree of imbalance. Second, the excess of magnetic energy persists in the whole inertial interval, however in quite a peculiar fashion. In both balanced and imbalanced cases, the residual energy spectrum has a power-law behavior close to $E_r(k_\perp) \propto k_\perp^{-2}$. In an inertial interval of limited extent, this leads to steepening of the magnetic spectrum and flattening of the velocity spectrum, however, the total energy scaling stays close to $-3/2$. Due to the relatively rapid spectral decline, the residual energy provides a subdominant contribution to both kinetic and magnetic energy spectra. We therefore propose that the mismatch between velocity and magnetic field energies becomes asymptotically irrelevant as the inertial range increases, in which case the universal scaling $-3/2$ is restored for both $E_v(k_\perp)$ and $E_b(k_\perp)$.

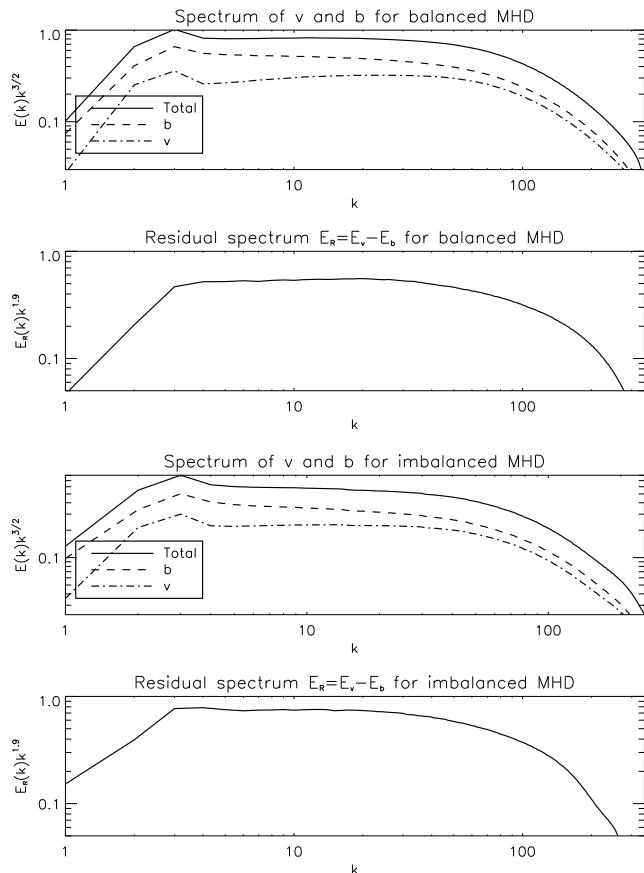


FIG. 1: Spectra of kinetic, magnetic, total, and residual energies in numerical simulations of balanced and imbalanced MHD turbulence.

Comparison with solar wind data.— Comparison of available numerical simulations with solar wind data is complicated by the fact that individual solar wind measurements typically last for a few correlation times ($\tau_c \sim 1$ hour), while in numerical simulations the spectra are averaged over tens or hundreds of turnover times to obtain good convergence. To make an appropriate comparison, we measure the velocity and magnetic field spectra for many individual simulation snapshots separated by about one eddy turnover time. We then plot distributions of the spectral indices obtained in this way for both balanced and imbalanced cases. The results are presented in Fig. (2).

For comparison, Fig. (3) presents analogous histograms obtained using solar wind measurements. The data from the *Advanced Composition Explorer* (ACE) spacecraft consists of 15,472 different spectra covering the 10 year period from 1998 to 2008 [16]. The data from the *Wind* spacecraft consists of those 120 of 176 spectra studied in [14] having the highest normalized cross-helicity $|\sigma_c| > 0.76$, that is, the greatest imbalance. The spectral indices are obtained from fits over the range of spacecraft frame frequencies from 10^{-3} to 3×10^{-2} Hz for the

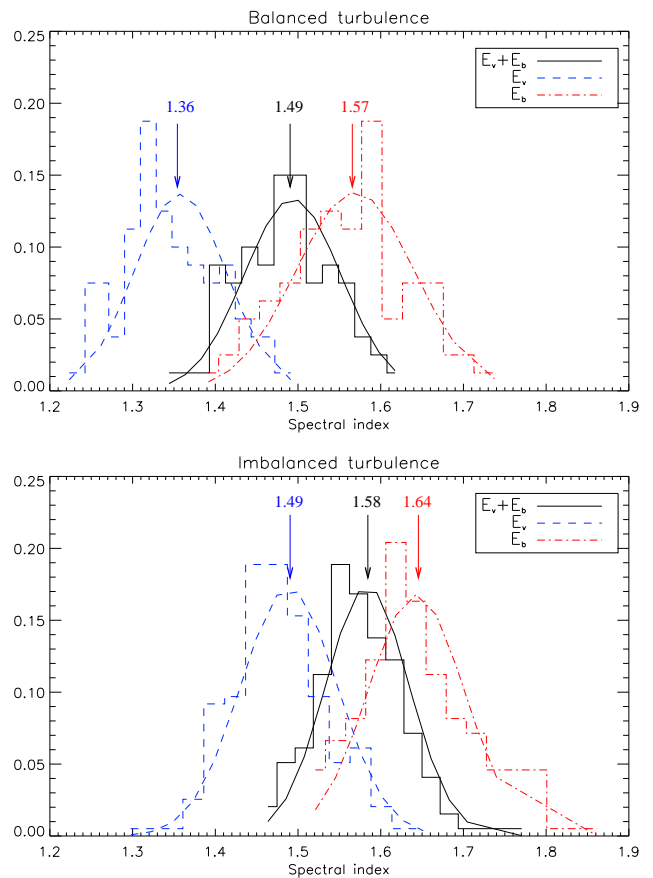


FIG. 2: Distributions of spectral indices for kinetic, magnetic, and total energies for individual snapshots in numerical simulations of MHD turbulence. Upper plot: balanced turbulence, 80 snapshots; lower plot: imbalanced turbulence, 196 snapshots. The average spectral indices are indicated by arrows. Normal distributions with the mean values and variances matching those of the data are also shown.

Wind data [14] and from 1.8×10^{-4} to 3.9×10^{-3} Hz for the ACE data [16]. It turns out that the scatter of individual indices in numerical simulations closely resembles the corresponding scatter in solar wind measurements. The excess of magnetic energy over kinetic energy is also seen in the solar wind where, in the study [14] for example, the power-law exponent of the residual energy takes typical values around 1.75. The solar wind also shows a tendency for the spectral indices of velocity and magnetic field to be closer together when the normalized cross-helicity is high than when it is low [14, 24]. A similar tendency is evident in the simulation results in Fig. 2. We therefore propose that the mismatch between $E_b(k_\perp)$ and $E_v(k_\perp)$ observed in the solar wind turbulence is neither the manifestation of non-universality of MHD turbulence nor does it indicate a breakdown of the applicability of incompressible MHD turbulence theory to the solar wind. Rather, it is a consequence of significant residual energy generated at large scales, in agreement

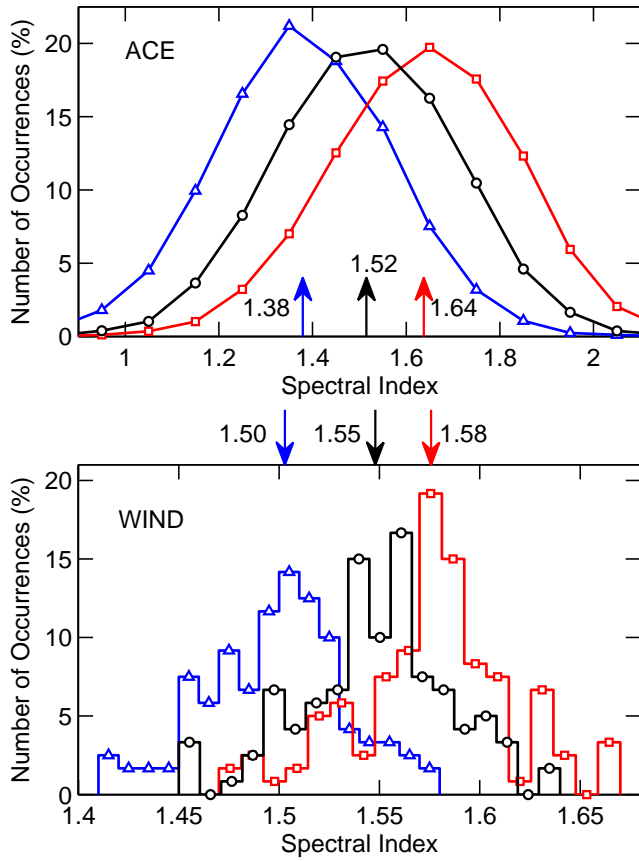


FIG. 3: Histograms of measured spectral indices for the velocity spectrum (blue triangles), magnetic field spectrum (red squares), and total energy spectrum (black circles) in the solar wind using data from the *ACE* and *Wind* spacecraft. The average spectral indices are indicated by the arrows. Note the different horizontal scales in the two plots.

with numerical simulations.

Conclusions.—Velocity spectra, magnetic field spectra, and total energy spectra in high resolution numerical simulations of 3D incompressible MHD turbulence are shown to be in good agreement with solar wind observations at 1 AU where the respective spectral indices of E_v , E_b , and E are approximately centered around 1.4-1.5, 1.6-1.7, and 1.5-1.6 [see, e.g., 13, 14, 16]. It is important to note that the large variability found in solar wind spectral indices is also observed in temporal snapshots of the numerical simulations. The unique scaling laws obtained by averaging simulation spectra over many eddy turnover times can also be obtained through a statistical analysis of the spectral indices of those snapshots. This provides justification for the widely used statistical approach to the analysis of spectral indices in the solar wind, where averaging over many turnover times is not practical. Our results indicate that universal inertial range dynamics may be present in the solar wind in spite of the observed high variability of solar wind measurements, and that solar wind turbulence spectra are con-

sistent with the characteristics of incompressible MHD turbulence.

This work was supported by the US DoE awards DE-FG02-07ER54932, DE-SC0003888, DE-SC0001794, the NSF grant PHY-0903872, and the NSF Center for magnetic Self-organization in Laboratory and Astrophysical Plasmas at U. Wisconsin-Madison. High Performance Computing resources were provided by the Texas Advanced Computing Center (TACC) at the University of Texas at Austin under the NSF-TeraGrid Project TG-PHY080013N. Work at Los Alamos was supported by the NASA Solar and Heliospheric Physics Program and the NSF SHINE Program.

-
- [1] D. Biskamp, *Magnetohydrodynamic Turbulence* (2003).
 - [2] R. M. Kulsrud, *Plasma physics for astrophysics* (2005).
 - [3] M. L. Goldstein, D. A. Roberts, and W. H. Matthaeus, *Ann. Rev. Astron. Astrophys.* **33**, 283 (1995).
 - [4] C. Tu and E. Marsch, *Space Sc. Rev.* **73**, 1 (1995).
 - [5] R. Bruno and V. Carbone, *Living Reviews in Solar Physics* **2**, 4 (2005).
 - [6] J. Maron and P. Goldreich, *Astrophys. J.* **554**, 1175 (2001), arXiv:astro-ph/0012491.
 - [7] W. Müller and R. Grappin, *Physical Review Letters* **95**, 114502 (2005), arXiv:physics/0509019.
 - [8] J. Mason, F. Cattaneo, and S. Boldyrev, *Physical Review Letters* **97**, 255002 (2006), arXiv:astro-ph/0602382.
 - [9] J. Mason, F. Cattaneo, and S. Boldyrev, *Physical Review E* **77**, 036403 (2008), 0706.2003.
 - [10] J. C. Perez and S. Boldyrev, *Physical Review Letters* **102**, 025003 (2009), 0807.2635.
 - [11] J. C. Perez and S. Boldyrev, *Astrophys. J. Lett.* **710**, L63 (2010), 0912.0901.
 - [12] J. J. Podesta, D. A. Roberts, and M. L. Goldstein, *Astrophys. J.* **664**, 543 (2007).
 - [13] J. A. Tessein, C. W. Smith, B. T. MacBride, W. H. Matthaeus, M. A. Forman, and J. E. Borovsky, *Astrophys. J.* **692**, 684 (2009).
 - [14] J. J. Podesta and J. E. Borovsky, *Physics of Plasmas* **17**, 112905 (2010).
 - [15] C. H. K. Chen, A. Mallet, T. A. Yousef, A. A. Schekochihin, and T. S. Horbury, *ArXiv e-prints* (2010), 1009.0662.
 - [16] J. E. Borovsky, submitted to *J Geophys. Res.* (2011).
 - [17] S. Galtier, S. V. Nazarenko, A. C. Newell, and A. Pouquet, *Astrophys. J. Lett.* **564**, L49 (2002).
 - [18] S. Galtier and B. D. G. Chandran, *Physics of Plasmas* **13**, 114505 (2006).
 - [19] J. C. Perez and S. Boldyrev, *Astrophys. J. Lett.* **672**, L61 (2008), 0712.2086.
 - [20] B. B. Kadomtsev and O. P. Pogutse, *Soviet Journal of Experimental and Theoretical Physics* **38**, 283 (1974).
 - [21] H. R. Strauss, *Physics of Fluids* **19**, 134 (1976).
 - [22] W. Müller, D. Biskamp, and R. Grappin, *Physical Review E* **67**, 066302 (2003), arXiv:physics/0306045.
 - [23] A. Pouquet, U. Frisch, and J. Leorat, *Journal of Fluid Mechanics* **77**, 321 (1976).
 - [24] J. E. Borovsky and M. H. Denton, *Journal of Geophysical Research (Space Physics)* **115**, 10101 (2010).